# Beta spectrometry with metallic magnetic calorimeters in the framework of the European EMPIR project MetroBeta

M. Loidl[a,*], J. Beyer[b], L. Bockhorn[c], C. Enss[d], S. Kempf[d], K. Kossert[c], R. Mariam[a], O. Nähle[c], M. Paulsen[b], P. Ranitzsch[c], M. Rodrigues[a], M. Schmidt[b]

[a] CEA, LIST, Laboratoire National Henri Becquerel (LNE-LNHB), CEA-Saclay, 91191, Gif sur Yvette Cedex, France
[b] Physikalisch-Technische Bundesanstalt (PTB), Abbestrasse 2-12, 10587, Berlin, Germany
[c] Physikalisch-Technische Bundesanstalt (PTB), Bundesallee 100, 38116, Braunschweig, Germany
[d] Kirchhoff-Institute for Physics, Heidelberg University, Im Neuenheimer Feld 227, 69120, Heidelberg, Germany

## HIGHLIGHTS

- Beta spectrometry using metallic magnetic calorimeters was developed in the European Metrology Research Project MetroBeta.
- New source/absorber preparation techniques and a new detector module have been developed.
- High statistics measurements of the beta spectra of $^{151}$Sm, $^{14}$C and $^{99}$Tc were performed; measurements of $^{36}$Cl will follow.

## ARTICLE INFO

## ABSTRACT

The aim of the European Metrology Research Project MetroBeta is to improve the knowledge of the shapes of beta spectra, both in terms of theoretical calculation and measurement. The precise knowledge of beta spectra is required for the activity standardisation of pure beta emitters. Metallic magnetic calorimeters (MMCs), a type of cryogenic detectors, with the beta emitter embedded in the absorber have proven to be among the best beta spectrometers, in particular for low-energy beta transitions. Within this project, new designs of MMCs optimized for five different beta energy ranges were developed and a new detector module was constructed. The beta spectra of $^{151}$Sm, $^{14}$C and $^{99}$Tc have been measured so far; additional measurements with $^{36}$Cl are under preparation. Improved theoretical calculation methods and complementary measurement techniques complete the project.

## 1. Introduction

There are several fields of research and application that request better knowledge of beta spectrum shapes and maximum beta energies. In the field of radionuclide metrology, precise data on beta spectra are essential for the calculation of the detection efficiency for absolute activity measurement of pure beta emitters, in particular by liquid scintillation counting (see, e.g., Kossert and Mougeot, 2015). Hence, they are a prerequisite for the realization of the activity unit Bq for these nuclides. Nuclear medicine introduces more and more beta emitters for local tumor irradiation with the aim of limiting the damage to unimpaired tissue. The calculation of the administered dose on the level of individual cells depends crucially on the beta spectrum shape. In the nuclear power industry, the mean energy of beta emissions, resulting from the shapes and the endpoints of beta spectra, is important

for the calculation of the remnant heat in reactor cores upon reactor shutdown. Also, nuclear waste management can be made more cost-efficient if better decay data on the numerous beta emitters present in the waste are available.

In principle, there are two ways to determine the shapes of beta spectra: theoretical calculation or experimental beta spectrometry. Neither of them is trivial. Calculations of spectra from forbidden (higher than first order), in particular non-unique transitions are very complicated and spectra published in literature often reveal large discrepancies for one and the same radionuclide.

In terms of experimental beta spectrometry, spectral distortions can arise both from insufficiencies of the spectrometers themselves (e.g. due to low energy resolution, non-linear response in energy or energy-dependent detection efficiency) and from energy loss of the beta particles in the source ("self-absorption") and other materials. Magnetic and

**Table 1**

References on experimental determinations of the $^{99}$Tc beta spectrum. All measurements are suffering from a high energy threshold of about 50 keV or more.

| Method | Energy range | Reference |
| --- | --- | --- |
| Magnetic spectrometer | > 140 keV | Taimuty (1951) |
| Magnetic spectrometer | > 50 keV | Feldman and Wu (1952) |
| Plastic scintillation detector | > 50 keV | Snyder and Beard (1966) |
| 4π Si(Li) | 55 keV–250 keV | Reich and Schüpferling (1974) |

electrostatic spectrometers can in principle provide precise beta spectra, but require intense sources, bringing along spectrum distortion due to strong self-absorption. Otherwise the count rate is very low, demanding very long measurement times and efficient dark count suppression. The energy resolution of semiconductor detectors is sufficient for beta spectrometry; however, they suffer from energy dependent electron backscattering from the detector surface, from energy loss of the beta particles in the dead layer and also from self-absorption in the source. Beta emitters have already been implanted into semiconductor detectors. In this case, the above-mentioned problems do not occur, but the performance of the detector is degraded by the additional dopant (e.g. Laegsgaard et al., 1984) and the fabrication of a dedicated semiconductor detector to measure just one beta spectrum is rather costly. None of these techniques is adapted to a systematic study of beta spectrum shapes.

The fact that the above-mentioned techniques are suffering from a rather high energy threshold is demonstrated in Table 1, which compiles references concerning measurement of the beta spectrum of $^{99}$Tc. In none of these experiments the important low-energy part below 50 keV could be measured.

Metallic magnetic calorimeters (MMCs) are a particular type of cryogenic detectors operating at very low temperature, usually between 10 mK and 50 mK (Enss et al., 2000; Fleischmann et al., 2005; Kempf et al., 2018). MMCs with beta emitters enclosed in noble metal absorbers have demonstrated their potential for the study of beta spectrum shapes in recent years (Rotzinger et al. 2008; Loidl et al. 2010, 2014). In the project MetroBeta (EMPIR, 2016), MMCs have been adapted to the requirements for low to medium energy (few keV to ∼ 1 MeV) beta spectrometry, and three beta spectra, covering different types of beta transition and a range of Q values between ∼ 70 keV and 300 keV, have been measured: $^{151}$Sm (1$^{st}$ forbidden non-unique; $Q = 76.4$ keV), $^{14}$C (allowed; $Q = 156.476$ keV) and $^{99}$Tc (2$^{nd}$ forbidden non-unique; $Q = 293.8$ keV). Measurements of $^{36}$Cl (2$^{nd}$ forbidden non-unique; $Q = 709.53$ keV) are not yet completed as high-energy beta emitters ($Q > 500$ keV) generate bremsstrahlung within the metal absorbers. As part of the generated photons escape from the detector, the corresponding events are shifted to a lower energy part of the spectrum and the measured spectrum becomes slightly distorted. This issue will be resolved by utilizing novel bilayer absorbers that combine the properties of two different metals to suppress the energy loss due to bremsstrahlung emission.

Other work packages of the project address improved theoretical beta spectra calculation methods and complementary measurement techniques.

The following sections describe the development of the MMCs, the source/absorber preparation techniques, and the measurements that have been accomplished so far within the project.

## 2. Metallic magnetic calorimeter development for beta spectrometry

Within this project, MMCs have been designed specifically to match the requirements of beta spectrometry (Loidl et al., 2018). The MMCs are designed for the attachment of an absorber with the radionuclide embedded inside. For optimal performance, the MMC design must be
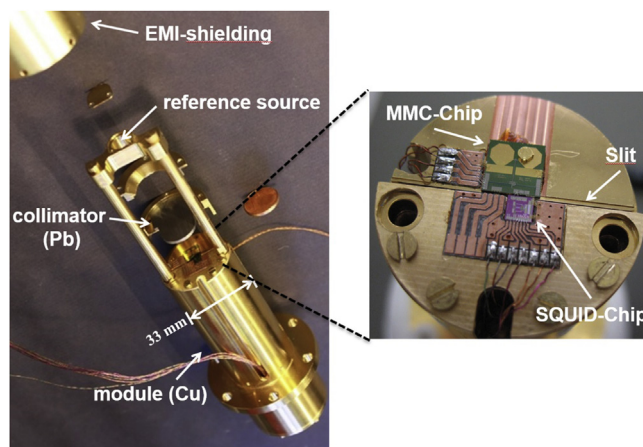


**Fig. 1.** MMC detector module. (Color figure online)

adapted to the heat capacity of the radiation absorber, i.e. the material and dimensions of the absorber and the operating temperature. High-purity gold (5N or 6N) is usually the absorber material of choice, but under special circumstances other materials or material combinations may be used. The heat capacity should be kept as small as possible for highest energy resolution and lowest energy threshold. Monte Carlo simulations are performed for each beta emitter to determine the minimal absorber thickness required to stop all beta particles up to the beta endpoint energy. Based on optimization calculations, MMCs were designed to match five absorber heat capacities, enabling to span a range of beta spectra with Q values (∼20 keV–∼1 MeV) covering the majority of the beta spectra of interest. MMCs of all five sizes were micro-fabricated on common wafers.

A new detector module, shown in Fig. 1, was designed for the beta spectra measurements. In addition to the MMC itself and the SQUID (Super Conducting Quantum Interference Device, see e. g. Clarke and Braginski, 2005) used for the MMC signal readout, it can host a collimator and a radionuclide photon source with variable distance to the absorber for energy calibration, linearity check and response stabilization.

## 3. Source preparation techniques

The source preparation is crucial for the precise measurement of beta spectra with MMCs. The radioactive material must be completely embedded into an absorber consisting of an appropriate material to ensure that every beta particle is detected, and the entire energy is deposited and thermalized, i. e. transformed to heat. Within the framework of this project, the radioactive material was deposited by two different methods, electrodeposition as well as drop deposition, either directly onto the absorber material or onto a separate source carrier foil. To enclose the sources inside the absorber and realize a 4π geometry, in the first case a second foil of absorber material was placed on top of the first foil with the source, in the second case the source carrier foil was sandwiched between bottom and top absorber foils. Each stack of foils was then bonded together by diffusion welding. Temperature, pressure and processing time were varied to fabricate the 4π source/absorber assemblies. The parameters to obtain reliable enclosure were found to depend strongly on the absorber material as well as on the radionuclide and the chemical composition of the source material.

The best source preparation approach - besides implanting the radionuclide directly into the absorber material - is a metallic layer formed by electrodeposition, as long as this is possible for the considered element. In many cases, an oxide/hydroxide layer may form during electrodeposition. This can still be a good quality source consisting in a very thin, homogenous layer. In the past, some experience has been gained with electrodeposition of beta emitters for MMC-based

measurements, both forming metal ($^{63}$Ni) and oxide/hydroxide ($^{241}$Pu) layers (Loidl et al. 2014). Within this project, a $^{151}$Sm source was electrodeposited on a silver foil, forming a Sm oxide/hydroxide layer. Also $^{99}$Tc was electrodeposited; the deposit is barely visible but, according to the adopted electrodeposition procedure, should be metallic technetium.

Where electrodeposition is not possible, as in the case of $^{14}$C or $^{36}$Cl, drop-deposited sources were produced. Typical radionuclide solutions contain certain salt loads, which means that drop deposition often leads to the formation of large (of order of micrometers) salt crystals. Previous studies have revealed that salt crystals can cause considerable spectrum distortion due to incomplete thermalization (Le-Bret et al., 2012). One approach to avoid the formation of large salt crystals is to decrease the individual drop size to a few picolitres, and to deposit a number of droplets corresponding to the required activity in a 2D-array pattern. Commercial micro-dispensing systems can deposit single droplet volumes of less than 50 pl in combination with a placement accuracy of better than 20 μm. With the help of an automated micro-dispensing system different radionuclide solutions ($^{36}$Cl, $^{99}$Tc, and $^{14}$C) were deposited onto gold foils. Milling techniques were used to format gold foils into an array of absorber elements with lateral dimensions of about 0.7 mm and 1.6 mm. Fig. 2a shows an absorber array after the radioactive solution was dried. Here, volumes of 100 nl (left half) and 50 nl (right half) of a $^{99}$Tc solution were deposited in the middle of each marked absorber. The fact that the deposit is not visible indicates the absence of large crystallizations. Checking the activity by visual inspection is hence not possible but based on the results of an autoradiographic image, see Fig. 2b, the positions and the different activities of the deposited material were confirmed. The quality of a drop-deposited source, prepared with a micro-dispensing system, can be demonstrated by comparing its measured spectrum with that of an electroplated source.

Fine dispersion of the source material in the absorber metal will also improve the source quality compared to a conventional drop-deposited source. One technique resulting in fine dispersion consists in alternate folding and laminating of the foil with the source deposit. This breaks the source crystals into tens of nanometer small particles that are embedded in the metal foil (Hoover et al., 2015). Since, after this mechanical processing, the activity is dispersed in the entire foil volume, this source foil must then be sandwiched between two metal foils of the required thickness. This technique was applied to the electrodeposited $^{151}$Sm source, because its layer was blackish and was considered not to be ideally thin. Another technique resulting in fine dispersion consists in the absorption of radionuclide solutions into nano-porous metal samples. In the context of $Q$ spectroscopy of alpha emitters (Rodrigues et al., 2018), deposition of actinide solutions into gold nanofoam (Sun and Balk, 2008), constraining the crystals to the pore size of tens of nanometers, is also being studied. The gold nanofoam has been prepared by de-alloying a gold-silver alloy with phosphoric acid. The pore size can be controlled via the concentration and the temperature of the etchant and the etching time.

Novel bilayer absorbers are being developed, in order to measure the beta spectrum of $^{36}$Cl ($Q = 709.53$ keV) which suffers from distortion due to bremsstrahlung escape when pure gold absorbers are employed. The distortions are reduced by embedding the radionuclide into $2 \times 150$ μm copper foils ($Z = 29$) and adding additional $2 \times 200$ μm gold foils ($Z = 79$) around the copper. While the copper layers lead to less bremsstrahlung generation and reduce the energy of the emitted beta particles, the high stopping power of the surrounding gold layers fully stops the electrons while keeping the overall absorber dimensions and the related heat capacity small. Preparing this kind of absorbers requires several steps of diffusion welding in an oxygen-free oven to avoid the oxidation of the copper.

## 4. Beta spectrum measurements

So far, three beta spectra have been measured using MMCs within the MetroBeta project; as already mentioned, the more challenging measurement of the spectrum of $^{36}$Cl is under preparation.

### 4.1. $^{14}$C

The spectrum of $^{14}$C has been measured using a source prepared by conventional drop deposition, but from a carrier-free, high specific activity solution. After drying, the deposit was invisible, even under an optical microscope, so the source can be considered to be of high quality. It was deposited on a 25 μm thick gold foil, thick enough to stop all beta particles up to the end point of the spectrum (156.5 keV). Since the $^{14}$C atoms are bound in a volatile organic compound, diffusion welding is not a viable option for source enclosure. The foil with the source was just folded over and slightly pressed. Gold is highly ductile and keeps its shape once folded; no beta electrons can escape from being absorbed in the gold absorber. Gold is a good thermal conductor at very low temperature, so the thermal contact between the two halves of the absorber through the bending is sufficient. The absorber (Au, 1 mm$^2 \times (2 \times 25$ μm)) was placed on an MMC chip whose size best matches its heat capacity ($C_{abs} = 67$ pJ/K at 20 mK). The experimental conditions during the spectrum measurement were far from optimal.
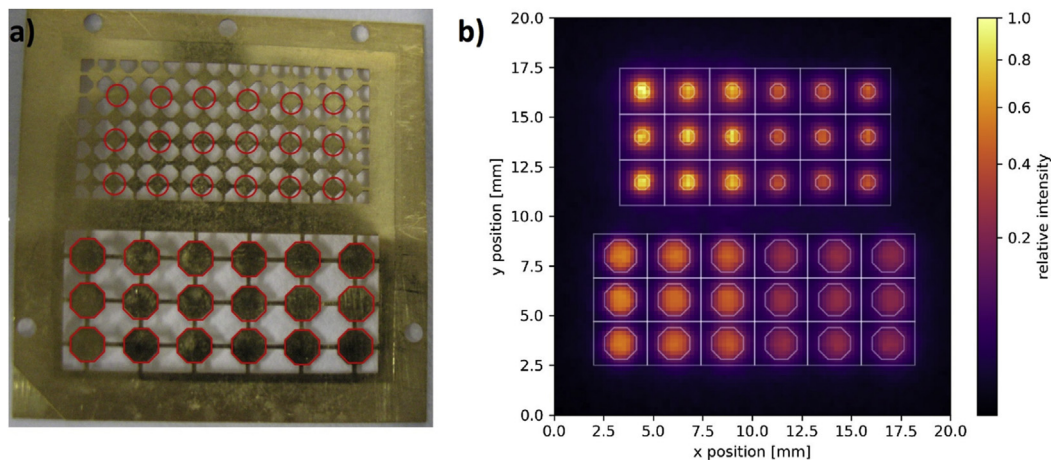


**Fig. 2.** a) Photograph of an array of pre-fabricated gold absorber foils with $^{99}$Tc sources deposited by a microdrop dispenser system in the middle of the marked absorbers. b) Autoradiographic image of the same array. Two different activities, 5 Bq/2.5 Bq, have been deposited on each marked absorber in the left/right half of the array. The activity is well centered on each absorber. (Color figure online)
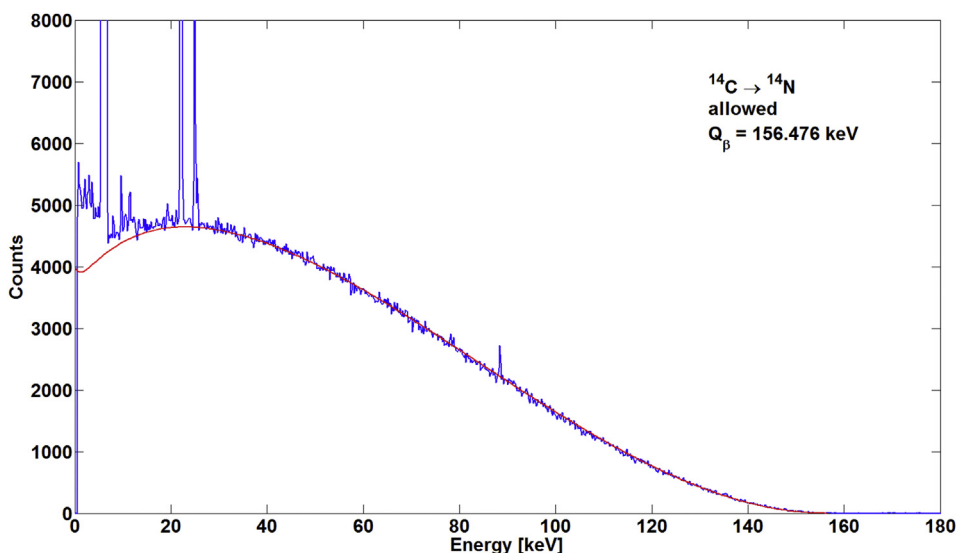
**Fig. 3.** Beta spectrum of $^{14}$C measured with an MMC (blue). The lines at 22 keV, 25 keV and 88 keV are K X-ray and gamma ray lines from an external $^{109}$Cd source and the broad line at around 6 keV, in reality a clipped double line, is the K α + β line of an external $^{55}$Fe source, these lines are used for energy calibration. The weak lines at around 10 keV are escape lines. The red line is a theoretical spectrum calculated with the code BetaShape. The increase of the experimental spectrum at low energies may be due to the degraded detector performance; a new measurement under improved conditions should clarify this question. (Color figure online). (For interpretation of the references to colour in this figure legend, the reader is referred to the Web version of this article.)

During the cooling phase, the glue layer fixing the MMC chip to its holder broke, the chip was then only suspended by the aluminum and gold bonding wires used for electric and thermal contacts. This had two consequences degrading the detector performance. One of them is that the thermal time constant of the detector was longer than expected, leading to a large fraction – more than 50% – of piled-up pulses that had to be removed from the data set. The major part of pile-up is removed by applying an extendable dead-time. A cut on the chi-square of the optimal filter used for the pulse-height determination removes practically all remaining piled-up events, too closely spaced in time to be detected separately and removed by the dead-time. The chi-square criterion is a measure for deviations of the pulse shape from the normal one. After 10 days of data acquisition at a rate of ~7 counts per second, the final spectrum, shown in Fig. 3, contains 2.7 million events. The other consequence is that the MMC could vibrate, resulting in an energy resolution near 200 eV (FWHM), about a factor 5 worse than expected from the absorber heat capacity. Nevertheless, the detector performance was much better than in the measurement published in Loidl et al. (2018): The energy resolution was improved by a factor five, while the energy threshold was reduced from ~5 keV to ~700 eV. Fig. 3 shows also a theoretical spectrum calculated with the code BetaShape (Mougeot and Bisch, 2014; Mougeot, 2015). The deviation of the experimental spectrum at low energies may be attributed to the degraded detector performance. The measurement will be repeated after regluing the MMC chip to fully exploit the performance that can be expected from the MMC.

### 4.2. $^{151}$Sm

A $^{151}$Sm source was electrodeposited on a 10 μm thick silver foil. After the mechanical processing described in section 3, this source foil (0.8 mm × 0.8 mm × 7 μm) was sandwiched between two silver foils (0.9 mm × 0.9 mm × 15 μm each) and the three foils were diffusion-welded to form the absorber (heat capacity: 29 pJ/K at 20 mK). The performance of the MMC during this measurement was as expected. An energy resolution ranging from about 45 eV (FWHM) at 6 keV to 70 eV at 25 keV and an energy threshold of 250 eV were observed. It should be mentioned here that under optimal conditions the energy resolution of an MMC is nearly independent of energy since it is only limited by noise. Various effects like temperature fluctuation of the thermal bath can, however, introduce some energy-dependent terms. The thermal time constant (1/e) of the detector was 460 μs; at a count rate of 8.7 s$^{-1}$, the fraction of piled-up pulses was very low. After 14 days of data acquisition, the spectrum contains 10.2 million events after

pile-up suppression.

$^{151}$Sm is the only non-pure beta emitter measured within the MetroBeta project: It has a main β$^-$ decay branch ($Q_\beta$ = 76.3 keV) to the ground state and a second β$^-$ decay branch to the 21.54 keV excited level of $^{151}$Eu. Both transitions are first forbidden non-unique. The recommended values for the respective probabilities of the two decay paths are 99.07 (4) % and 0.93 (4) % (Bé et al., 2016). The de-excitation of the 21.54 keV excited state is highly converted; only 3.4% of the gamma transition lead to the emission of gamma-rays (total probability: 3.24 (13) × 10$^{-4}$), the rest leads to the emission of conversion electrons and subsequently X-rays and/or Auger electrons. The detector absorber with its given dimensions, sufficient to stop all beta electrons up to the beta $Q$ value, does also stop all conversion electrons, more than 99% of all X-rays and more than 95% of the 21.54 keV gamma photons. The result is that for practically all beta decays to the excited level the sum of the beta energy and the gamma energy is absorbed. So the measured spectrum for the decays to the excited level is shifted by the energy of the gamma transition and starts at 21.54 keV, leading to a step in the recorded spectrum. Since the maximum energy for this beta branch equals the $Q$ value minus the gamma transition energy, the end point of both measured spectra is the same, 76.3 keV. As it is not possible to distinguish events from the two decay branches, both spectra are superimposed in one experimental spectrum.

The measured spectrum is shown in Fig. 4 together with theoretical spectra calculated with the code BetaShape (Mougeot and Bisch, 2014; Mougeot, 2015) for both decay paths. The spectrum corresponding to the decay to the ground state was fitted to the experimental spectrum in the energy range from 10 keV to 20 keV. It can clearly be seen that above 21.5 keV the experimental spectrum lies higher than the fitted spectrum of the main decay branch. The spectrum corresponding to the decay to the excited level was shifted by 21.54 keV and fitted to the experimental spectrum in the energy range 26 keV–40 keV. The area lying between the two theoretical spectra, corresponding to the probability of the decay to the excited state of $^{151}$Eu, amounts to 2.6% of the total. We do not state any uncertainty on the measured probability, firstly because the theoretical spectra are preliminary, secondly because the theoretical spectrum does not fit the experimental spectrum below 6 keV, and thirdly because the fitting procedure was rather coarse. Nevertheless, this value is in clear contradiction with the recommended value for the probability of the decay to the $^{151}$Eu excited level. Concerning the beta spectrum shape, the discrepancy between experiment and theory at low energies is most likely due to an incomplete control of the atomic effects in the theoretical calculation of this first forbidden, non-unique transition.
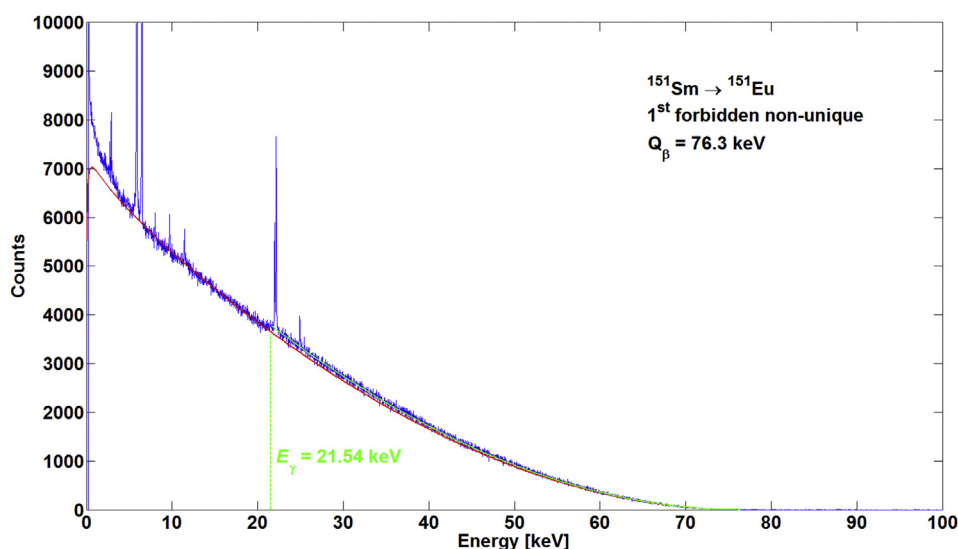
**Fig. 4.** Beta spectrum of $^{151}$Sm measured with an MMC (blue) together with theoretical spectra calculated for the two beta decay branches, to the ground state (red) and to the 21.54 keV excited level of $^{151}$Eu (green). The spectrum from the transition to the excited state is shifted towards higher energies by 21.54 keV, the energy of the gamma transition that is detected in sum with the beta particle energy. Therefore both measured spectra end at the same energy, 76.3 keV. The energy calibration was performed with an external X-ray source composed of $^{55}$Fe and $^{109}$Cd. (Color figure online). (For interpretation of the references to colour in this figure legend, the reader is referred to the Web version of this article.)
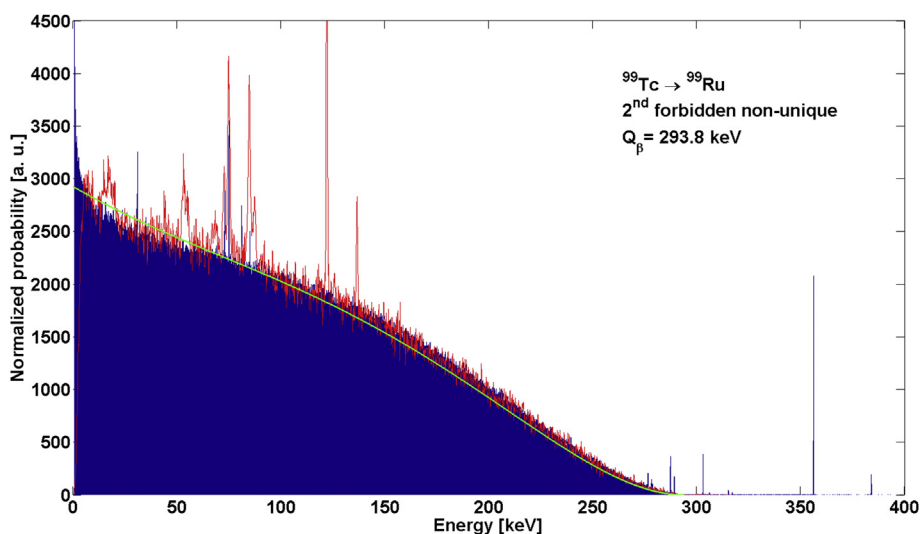


**Fig. 5.** Beta spectrum of $^{99}$Tc measured with $^{99}$Tc sources fabricated in two different ways, with two independent MMCs, in different setups and using different data analysis routines. For better visibility, one spectrum is represented as a histogram (blue, measured at LNHB) and the other one as a line (red, measured at PTB). The energy calibration was performed with a $^{133}$Ba source (LNHB) respectively a $^{57}$Co source (PTB). A theoretical spectrum calculated with the code BetaShape is also shown (green). (Color figure online). (For interpretation of the references to colour in this figure legend, the reader is referred to the Web version of this article.)

### 4.3. $^{99}$Tc

The beta spectrum of $^{99}$Tc was measured both at PTB and at LNHB. What makes this comparison interesting is that these measurements are completely independent. The technetium sources were prepared by different techniques and are of different chemical composition. The MMCs were mounted in different detector modules. The measurements used different cryogenic setups in different electromagnetic environment. Data were recorded by different data acquisition systems, and data analysis was performed using different routines.

At LNHB, a $^{99}$Tc source was electrodeposited on a 10 μm thick gold foil. The deposit is extremely thin and should be metallic technetium. However, the deposition yield and the resulting activity per surface area were lower than expected. Therefore a sufficiently large piece of this foil had to be folded three times to reduce its area to a size (~0.5 mm × 0.7 mm) small enough to enclose it in an MMC absorber. This source foil was then sandwiched between two gold foils (0.9 mm × 0.9 mm × 74 μm each) and this stack was diffusion welded. The final absorber had a heat capacity of 350 pJ/K at 20 mK, much larger than the previous detectors. The pulses had a rise time (10%–90%) of 14 μs and a decay time (1/e) of 2.15 ms. Data was acquired during 13.7 days and the spectrum contains 5.65 million events. The energy resolution is practically energy-independent, about 100 eV (FWHM) up to 384 keV, the highest energy gamma line of a $^{133}$Ba source

used for energy calibration and check of the linearity. Comparing the measured and the tabulated line energies between 31 keV and 384 keV shows no larger deviations than 70 eV, less than the energy resolution, and no obvious trend.

At PTB, a $^{99}$Tc source was prepared with a micro-drop dispenser directly on a 90 μm thick gold foil formatted to an array of absorber elements with lateral dimensions of about 1.6 mm and 0.7 mm, shown in Fig. 2a. An identical foil was diffusion welded onto the first foil with the dried radioactive material. One of the larger source/absorber assemblies with an expected activity of about 5 Bq was selected and glued onto a matching MMC. The heat capacity of the absorber assembly is 545 pJ/K at 20 mK. The observed pulses had a rise time (10%–90%) of 31 μs and a decay time (1/e) of 4.6 ms. The data acquisition took 42 h and the resulting spectrum consisted of 0.5 million events with an energy threshold of about 5 keV. A $^{57}$Co source was used for energy calibration and the 122 keV gamma line showed an energy resolution of 600 eV (FWHM). The larger absorber and total heat capacity of the setup, as well as experimental problems with the temperature stability of the thermal bath explain the degraded energy resolution and threshold compared to the measurement performed at LNHB.

Fig. 5 shows a superposition of both experimental spectra. It is clear that the spectrum shape is practically the same. This spectrum shape will be a valuable input for the improvement of the theoretical calculation for this type of transition, 2$^{nd}$ forbidden non-unique. The

theoretical spectrum that is also shown in Fig. 5 has been calculated with the current version of the code BetaShape, supposing an allowed transition, and multiplied with an experimental shape factor (Reich and Schüpferling, 1974). It is not surprising that this shape factor, derived from a measurement with an energy threshold at 55 keV, cannot correctly reproduce the spectrum at lower energies. It is noteworthy that the spectrum measured at LNHB has an energy threshold of 650 eV.

## 5. Conclusions and perspectives

Within the European metrology project MetroBeta, developments of both MMCs and source/absorber preparation techniques for beta spectrometry using MMCs with beta emitters embedded in the absorber have been conducted. Several spectra resulting from different types of beta transition and with end-point energies ranging from ~76 keV to 294 keV have been measured and the spectrum of $^{36}$Cl (end-point energy 709 keV) will also be measured before the end of the project. The experimental spectra will be compared both with improved theoretical spectra calculated within the project, and with spectra obtained with complementary measurement techniques. The results presented in this work indicate a need for improved theoretical calculations, in particular for higher-order forbidden beta transitions. To this end, high-precision measurements using MMCs of further beta-emitting radionuclides are most desirable. Moreover, it was demonstrated that MMC measurements have also the potential to yield valuable information about other decay scheme parameters such as the probability of the beta decay from $^{151}$Sm to the excited level of $^{151}$Eu. Thus, MMC spectrometry applied to radionuclides with more complex decay schemes is considered as an interesting extended research field. Studies indicate that $^{129}$I, $^{204}$Tl and $^{210}$Pb are promising candidates for such measurements which should yield valuable nuclear decay data.

## Acknowledgements

## References

Bé, M.-M., Chisté, V., Dulieu, C., Kellett, M.A., Mougeot, X., Arinc, A., Chechev, V.P., Kuzmenko, N.K., Kibédi, T., Luca, A., Nichols, A.L., 2016. Table of Radionuclides. vol. 8 Monographie BIPM-5 13 978-92-822-2264-5.

Clarke, J., Braginski, A.I. (Eds.), 2005. The SQUID Handbook. Wiley VCH Verlag, Weinheim, Germany.
EMPIR, 2016. Website. http://metrobeta-empir.eu/.
Enss, C., Fleischmann, A., Horst, K., Schönefeld, J., Sollner, J., Adams, J.S., Huang, Y.H., Kim, Y.H., Seidel, G., 2000. Metallic magnetic calorimeters for particle detection. J. Low Temp. Phys. 121, 137–176.
Feldman, L., Wu, C.S., 1952. Investigation of the beta-spectra of $^{10}$Be, $^{40}$K, $^{99}$Tc, and $^{36}$Cl. Phys. Rev. 87, 1091–1099.
Fleischmann, A., Enss, C., Seidel, G., 2005. Metallic magnetic calorimeters. In: Enss, C. (Ed.), Cryogenic Particle Detectors. Topics Appl. Phys. 99. Springer Berlin/ Heidelberg, pp. 151–216.
Hoover, A.S., Bond, E.M., Croce, M.P., Holesinger, T.G., Kunde, G.J., Rabin, M.W., Wolfsberg, L.E., Bennett, D.A., Hays-Wehle, J.P., Schmidt, D.R., Swetz, D., Ullom, J.N., 2015. Measurement of the $^{240}$Pu/$^{240}$Pu mass ratio using a transition-edge-sensor microcalorimeter for total decay energy spectroscopy. Anal. Chem. 87, 3996–4000.
Kempf, S., Fleischmann, A., Gastaldo, L., Enss, C., 2018. Physics and applications of metallic magnetic calorimeters. J. Low Temp. Phys. 193, 365–379.
Kossert, K., Mougeot, X., 2015. The importance of the beta spectrum calculation for accurate activity determination of $^{63}$Ni by means of liquid scintillation counting. Appl. Radiat. Isot. 101, 40–43.
Laegsgaard, E., Andersen, J.U., Beyer, G.J., De Rújula, A., Hansen, P.G., Jonson, B., Ravn, H.L., 1984. The capture ratio N/M in the EC beta decay of $^{163}$Ho. In: Klepper, O. (Ed.), Proceedings of the 7th International Conference on Atomic Masses and Fundamental Constants AMCO-7, no. 26 in THD Schriftenreihe Wissenschaft und Technik 652-658, Darmstadt-Seeheim.
Le-Bret, C., Loidl, M., Rodrigues, M., Mougeot, X., Bouchard, J., 2012. Study of the influence of the source quality on the determination of the shape factor of beta spectra. J. Low Temp. Phys. 167, 985–990.
Loidl, M., Rodrigues, M., Censier, B., Kowalski, S., Mougeot, X., Cassette, P., Branger, T., Lacour, D., 2010. First measurement of the beta spectrum of $^{241}$Pu with a cryogenic detector. Appl. Radiat. Isot. 68, 1454–1457.
Loidl, M., Le-Bret, C., Rodrigues, M., Mougeot, X., 2014. Evidence for the exchange effect down to very low energy in the beta decays of $^{63}$Ni and $^{241}$Pu. J. Low Temp. Phys. 176, 1040–1045.
Loidl, M., Beyer, J., Bockhorn, L., Enss, C., Györi, D., Kempf, S., Kossert, K., Mariam, R., Nähle, O., Paulsen, M., Rodrigues, M., Schmidt, M., 2018. MetroBeta: beta spectrometry with metallic magnetic calorimeters in the framework of the european program of ionizing radiation metrology. J. Low Temp. Phys. 193, 1251–1256.
Mougeot, X., Bisch, C., 2014. Consistent calculation of the screening and exchange effects in allowed β$^-$ transitions. Phys. Rev. A 90, 1–8 012501.
Mougeot, X., 2015. Reliability of usual assumptions in the calculation of β and ν spectra. Phys. Rev. C 92, 059902 and Erratum: reliability of usual assumptions in the calculation of β and ν spectra Physical Review C 91, 055504. Phys. Rev. C 92, 059902.
Rodrigues, M., Laarraj, M., Loidl, M., Navick, X.-F., Mariam, R., 2018. Development of total decay energy spectrometry of α-emitting radionuclides using metallic magnetic calorimeters. J. Low Temp. Phys. 193, 1263–1268.
Rotzinger, H., Linck, M., Burck, A., Rodrigues, M., Loidl, M., Leblanc, E., Gastaldo, L., Enss, C., 2008. Beta spectrometry with magnetic calorimeters. J. Low Temp. Phys. 151, 1087–1093.
Snyder, R.E., Beard, G.B., 1966. Decay of $^{94}$Nb and $^{94m}$Nb. Phys. Rev. 147, 867–870.
Sun, Y., Balk, T.J., 2008. A multi-step dealloying method to produce nanoporous gold with no volume change and minimal cracking. Scr. Mater. 58, 727–730.
Taimuty, S.I., 1951. The beta-spectrum of $^{99}$Tc. Phys. Rev. 81, 461–462.